Bulletin of the Seismological Society of America, Vol. 73, No. 6, pp. 1685–1699, December 1983

A GENERALIZED REFLECTION-TRANSMISSION COEFFICIENT MATRIX AND DISCRETE WAVENUMBER METHOD FOR SYNTHETIC SEISMOGRAMS

BY Z. X. YAO AND D. G. HARKRIDER

ABSTRACT

Expressions for displacements on the surface of a layered half-space due to point force are given in terms of generalized reflection and transmission coefficient matrices (Kennett, 1980) and the discrete wavenumber summation method (Bouchon, 1981). The Bouchon method with complex frequencies yields accurate near-field dynamic and static solutions.

The algorithm is extended to include simultaneous evaluation of multiple sources at different depths. This feature is the same as in Olson's finite element discrete Fourier Bessel code (DWFE) (Olson, 1982).

As numerical examples, we calculate some layered half-space problems. The results agree with synthetics generated with the Cagniard-de Hoop technique, *P-SV* modes, and DWFE codes. For a 10-layered crust upper mantle model with a bandwidth of 0 to 10 Hz, this technique requires one-tenth the time of the DWFE calculation. In the presence of velocity gradients, where finer layering is required, the DWFE code is more efficient.

INTRODUCTION

Economic near-field solutions of a point source in a layered half-space are important in the fields of seismology and earthquake engineering. Recently, many approaches have been proposed to evaluate the layered half-space response. For example, there are generalized ray theory (Helmberger, 1968; Helmberger and Harkrider, 1978), reflectivity method (Fuchs and Muller, 1971), reflection and transmission coefficients matrix method (Kennett, 1974, 1980; Apsel, 1979; Kennett and Kerry, 1980), discrete wavenumber method (Bouchon, 1981), and discrete wavenumbers—finite element method (DWFE) (Olson, 1982), among others.

In this paper, a generalized reflection-transmission matrix and discrete wavenumber method for near-field synthetic seismograms is proposed. This approach is based on Kennett's reflection and transmission matrix method for the wavenumber integrands (1974, 1981) and the discrete wavenumber summation method (Bouchon, 1981) for the wavenumber integration. The reflection-transmission matrix is an effective procedure to evaluate the wavenumber integrand. Phase-delayed reflection and transmission coefficients are used which are slightly different than Kennett's expressions (1980). The algorithm includes simultaneous evaluation of the Green's functions of multiple sources at different depths.

INTEGRAND EXPRESSIONS

The displacement integrands on the free surface for buried source problems given by Kennett and Kerry (1979) in equation (5.22) are

$$W(0^+) = (M_U + M_D\tilde{R})[I - R_D^{RS}\tilde{R}]^{-1}T_U^{RS}[I - R_D^{SL}R_U^{FS}]^{-1}(R_D^{SL}\delta\Phi_D - \delta\Phi_U). \quad (1)$$

The notation used is that of Kennett and Kerry (1979). Slightly different relations are used for the reflection and transmission coefficients, which except for differences

in normalization, are given by their equation (4.26). The relations and additional definitions are found in the Appendix.

$\tilde{R}$ is the reflection coefficient matrix on the free surface, $(M_U + M_D\tilde{R})$ is the receiver function matrix (Helmberger, 1974).

$$\tilde{R} = \frac{1}{\Delta}\begin{pmatrix} \Omega_1^2 + a_1 b_1 & 2kb_1\Omega_1 \\ 2ka_1\Omega_1 & \Omega_1^2 + a_1 b_1 \end{pmatrix} \tag{2}$$

$$(M_U + M_D\tilde{R}) = \frac{1}{\Delta}\begin{pmatrix} k_{\beta_1}^2 ka_1 b_1 & k_{\beta_1}^2 b_1\Omega_1 \\ k_{\beta_1}^2 a_1\Omega_1 & k_{\beta_1}^2 ka_1 b_1 \end{pmatrix} \tag{3}$$

where

$$\Delta = k^2 a_1 b_1 - \Omega_1^2 \tag{4}$$

with

k = wavenumber,

α = P-wave velocity,

β = S-wave velocity,

μ = rigidity,

$k_\alpha = \omega/\alpha$,

$k_\beta = \omega/\beta$,

$a = \sqrt{k^2 - k_a^2}$, Re $a \geqq 0$,

$b = \sqrt{k^2 - k_\beta^2}$, Re $b \geqq 0$,

and

$$\Omega = k^2 - k_\beta^2. \tag{5}$$

R_D^{SL} is the generalized relection coefficient matrix for the P-SV waves between $z = z_s^+$ and $z = z_L^+$ (Figure 1). Using the relations for reflection and transmission coefficients given by Kennett (1974, 1980), and Kennett and Kerry (1979), we can calculate R_D^{SL} from

$$Q(z_s^+, z_L^+) = Q(z_s^+, z_{s+1}^+) \cdots Q(z_{L+1}^+, z_L^+) \tag{6}$$

with

$$Q(z_{K-1}^+, z_K^+) = \begin{pmatrix} \tilde{T}_U - \tilde{R}_D\tilde{T}_D^{-1}\tilde{R}_U & \tilde{R}_D\tilde{T}_D^{-1} \\ -\tilde{T}_D^{-1}\tilde{R}_U & \tilde{T}_D^{-1} \end{pmatrix} \tag{7}$$

where the submatrices correspond to the normalized reflection and transmission coefficients matrices given in the Appendix. R_D^{RS} and T_U^{RS} are the generalized reflection and transmission coefficient between $z = 0^+$ and $z = z_s^-$. R_U^{FS} is the

generalized reflection coefficient between $z = 0$ and $z = z_s^+$ and is calculated by the relation

$$R_U^{FS} = R_U^{RS} + R_D^{RS}\tilde{R}[I - R_D^{RS}\tilde{R}]^{-1}T_U^{RS}. \tag{8}$$

For *SH* waves, the displacement integrand on the free surface is as follows

$$V(0^+) = 2k(1 - R_{D,SH}^{RS})^{-1}T_{U,SH}^{RS}(1 - R_{D,SH}^{SL}R_{U,SH}^{FS})^{-1}(R_{D,SH}^{SL}\delta\chi_D - \delta\chi_V) \tag{9}$$

with the subscript denoting reflection and transmission coefficients appropriate for *SH* waves.

$\delta\Phi$ and $\delta\chi$ represent the source's terms which have been given by Langston and Helmberger (1975).

For many problems, a fault is treated as a summation of subfaults which can be considered point sources. Thus, there is need for rapid construction of Green's functions for several different source depths. Since the terms necessary for a given source depth calculations are obtained by the iterative relations of Kennett, we in effect calculate similar source depth terms for every interface above and below the

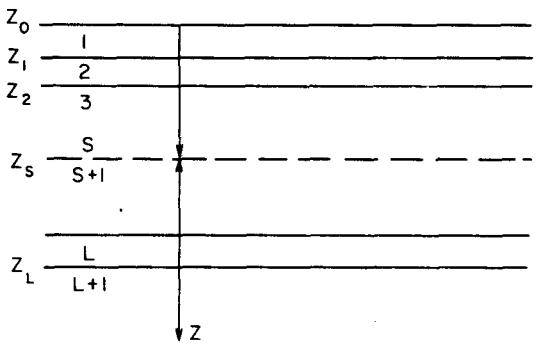

FIG. 1. Source and structure geometry.

source plane. The only additional effort for obtaining as many source depth Green's function as there are interfaces is in saving the intermediate values. This feature is similar to codes based on reciprocity, i.e., surface source and receiver at depth, such as DWFE (Olson, 1982) and PROSE (Apsel, 1979).

INTEGRAL SOLUTIONS

For a buried double couple, the free surface displacements are

$$\begin{aligned}
w(t) &= \frac{M_0}{4\pi\rho}\frac{d}{dt}\left[\dot{D}(t)^* \sum_{m=0}^{2} A_m(\lambda, \delta, \varphi)w_m(t)\right] \\
q(t) &= \frac{M_0}{4\pi\rho}\frac{d}{dt}\left[\dot{D}(t)^* \sum_{m=0}^{2} A_m(\lambda, \delta, \varphi)q_m(t)\right] \\
v(t) &= \frac{M_0}{4\pi\rho}\frac{d}{dt}\left[\dot{D}(t)^* \sum_{m=1}^{2} A_{m+3}(\lambda, \delta, \omega)v_m(t)\right]
\end{aligned} \tag{10}$$

where

$$A_0(\lambda, \delta, \varphi) = \tfrac{1}{2} \sin \lambda \sin 2\delta$$

$$A_1(\lambda, \delta, \varphi) = \cos \varphi \cos \lambda \cos \delta - \sin \varphi \sin \lambda \cos 2\delta$$

$$A_2(\lambda, \delta, \varphi) = \sin 2\varphi \cos \lambda \sin \delta + \tfrac{1}{2} \cos 2\varphi \sin \lambda \sin 2\delta$$

$$A_3(\lambda, \delta, \varphi) = 0$$

$$A_4(\lambda, \delta, \varphi) = -\cos \varphi \sin \lambda \cos 2\delta - \sin \varphi \cos \lambda \cos \delta$$

$$A_5(\lambda, \delta, \varphi) = \cos 2\varphi \cos \lambda \sin \delta - \tfrac{1}{2} \sin 2\varphi \sin \lambda \sin 2\delta. \tag{11}$$

φ = azimuth from the fault strike,

λ = rake angle,

δ = dip angle,

M_0 = seismic moment,

$\dot{D}$ = far-field time history.

ρ = density, and $w_m(t)$, $u_m(t)$, and $v_m(t)$ are step responses which correspond to the vertical, radical, and tangential displacements of three fundamental shear dislocations ($m = 2$, strike-slip fault; $m = 1$, dip-slip fault; $m = 0$, isotropic component of the 45° dip-slip fault). In the frequency domain they are as follows

$$w_m(\omega) = \int_0^\infty W_m J_m(kr) k \, dk$$

$$q_m(\omega) = \int_0^\infty \left[U_m J_m'(kr) - V_m \frac{m}{kr} J_m(kr) \right] k \, dk$$

$$v_m(\omega) = \int_0^\infty \left[U_m \frac{m}{kr} J_m(kr) - V_m J_m'(kr) \right] k \, dk \tag{12}$$

where

$$J_m'(x) = \frac{dJ_m}{dx}$$

$$\begin{pmatrix} U_m \\ W_m \end{pmatrix} = \frac{1}{\omega^4} (M_U + M_D \tilde{R})(I - R_U^{RS} \hat{R})^{-1} T_U^{RS} (I - R_D^{SL} R_U^{FS})^{-1} \cdot \left[R_D^{SL} \begin{pmatrix} P_m^+ \\ SV_m^+ \end{pmatrix} + \begin{pmatrix} P_m^- \\ SV_m^- \end{pmatrix} \right] \tag{13}$$

from (1)

$$V_m = \frac{2k}{\omega^4} (1 - R_{D,SH}^{RS})^{-1} T_{U,SH}^{RS} (1 - R_{D,SH}^{SL} R_{U,SH}^{FS}) (R_{D,SH}^{SL} SH_m^+ + SH_m^-) \tag{14}$$

from (9), with

$$\begin{array}{lll} P_0 = (2k_a^2 - 3k^2)/a & SV_0 = -\epsilon 3k & SH_0 = 0 \\ P_1 = \epsilon 2k & SV_1 = (2k^2 - k_\beta^2)/b & SH_1 = -\epsilon k_\beta^2/k \\ P_2 = k^2/a & SV_2 = -\epsilon k & SH_2 = k_\beta^2/b \end{array} \tag{15}$$

and

$$\epsilon = \begin{cases} -1 & \text{for } - \text{ superscript} \\ 1 & \text{for } + \text{ superscript.} \end{cases}$$

For an explosion type source,

$$w(t) = \frac{d}{dt}\,[\dot{\Psi}(t)^* w_0(t)]$$

$$q(t) = \frac{d}{dt}\,[\dot{\Psi}(t)^* q_0(t)] \tag{16}$$

where w_0 and q_0 are given as before from (12) and all the source coefficients are zero except

$$P_0 = \omega^2/a$$

and $\dot{\Psi}(t)$ is the reduced velocity potential of the explosion.

Wavenumber Integration

The Hankel transform-type integral representation of the displacements in the frequency domain involves quantities of the form

$$I_m = \int_0^\infty F(k, \omega) J_m(kr) k\, dk \quad m = 0, 1, 2. \tag{17}$$

The kernel $F(k, \omega)$ depends upon wavenumber, frequency source depth, and layer properties which we evaluate with generalized reflection and transmission coefficient matrices. Now, it is important to look for an efficient numerical integration scheme to handle the wavenumber integration.

Bouchon (1981) has demonstrated that the wavenumber integration (17) can be evaluated by a discrete wavenumber summation

$$I_m = \frac{\pi}{L} \sum_{j=0}^{\infty} \epsilon_j k_j F(k_j, \omega) J_m(k_j r) \tag{18}$$

$$\epsilon_j = \begin{cases} 2 & \text{for } j \neq 0 \\ 1 & \text{for } j = 0 \end{cases}$$

$$k_j = 2\pi j/L$$

if relations $r < L/2$ and $[(L - r)^2 + z^2]^{1/2} > \alpha t$ are satisfied. To avoid the influence of the singularities of the integrand $F(k, \omega)$, and the discretization, he gave to the

frequency an imaginary part, the effect of which is later removed from the time domain solution. In the numerical examples, the imaginary part of the frequency is the same as that given in Bouchon (1979). A discussion of its dependence on the time window and of the removal of its effect on the solution after Fourier transformation can be found in that paper.

TABLE 1

LAYER PARAMETERS FOR THE HALF-SPACE MODEL

h (km)	α (km/sec)	β (km/sec)	ρ (gm/cm^3)
∞	3.000	1.900	1.900

This discretization scheme is simpler than that used by the DWFE method (Olson, 1982). In the DWFE method, the discrete wavenumbers are determined by the roots of $J_0(kL)$ and $J_1(kL)$. An advantage of the Bouchon method over Kennett's wavenumber integration is that it is straightforward to obtain the near-field static solutions. The static contribution comes from zero frequency and is treated the

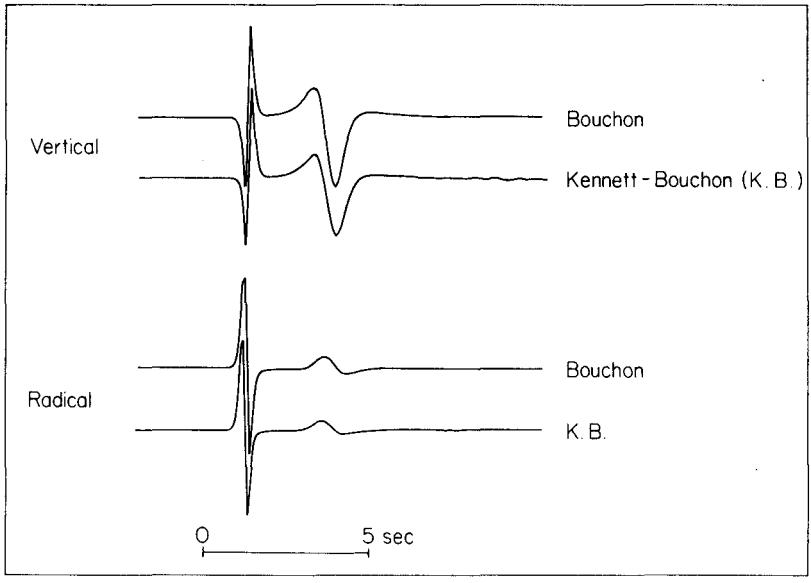

FIG. 2. Vertical and radial velocity record comparisons between an analytic and a three layer reflection-transmission coefficient calculation of an explosion in an homogeneous half-space.

same in Bouchon's technique as any other complex frequency. On the other hand, the slowness method requires special handling at zero frequency. The combination of Kennett's integrand algorithm with Bouchon's discrete wavenumber evaluation will be referred to as the Kennett-Bouchon (KB) algorithm.

The k loop is controlled by a previously specified precision e. If the ratio of the terms

$$|k_j F(k_j, \omega) J_m(k_j r)| \Big/ \left| \sum_{i=1}^{j} k_i F(k_i, \omega) J_m(k_i r) \right|$$

is less than e, the k loop stops. This condition must be met for every calculation in the loop. Since, at least one of the calculations will involve a Bessel function of

order one different than the others, the loop will not be terminated by a zero of the Bessel functions. As one might expect, the higher the frequency the larger the number of k terms required for convergence.

TABLE 2
LAYER PARAMETERS FOR THE CRUST HALF-SPACE MODEL

h (km)	α (km/sec)	β (km/sec)	ρ (gm/cm^3)
∞	6.200	3.500	2.700

NUMERICAL EXAMPLES

As a first numerical example, we calculate the vertical and radial velocity field at the free surface due to an explosion source in a homogeneous half-space (Table 1). Taking $r = 10$ km, $h = 1.2$ km, $\Delta t = 0.05$ sec, and $L = 100$ km, we obtain the

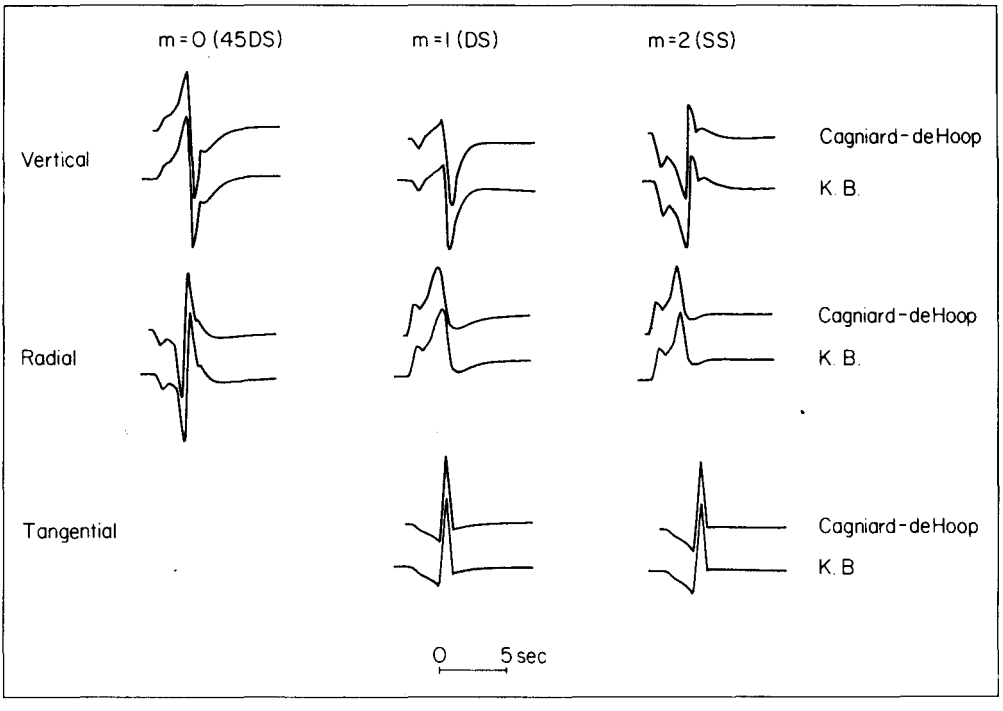

FIG. 3. Vertical, radial, and tangential displacement comparisons between Cagniard-de Hoop and the KB techniques for a dislocation in an homogeneous half-spaces. The records are for the three fundamental fault orientations at a range of 16 km.

velocities shown at the bottom of each pair in Figure 2. The calculation used the reflection and transmission coefficients generated by a three layer model of the homogeneous half-space. The upper trace for each velocity component of Figure 2 is calculated from the explicit discrete wavenumber expressions of Bouchon (1981). The differences of amplitude are only in the third decimal place.

In the second example, we calculate the displacements of a dislocation source in another half-space model (Table 2) and compare with ray theory using the Cagniard-de Hoop technique. These are shown in Figures 3 and 4; the top traces of each pair

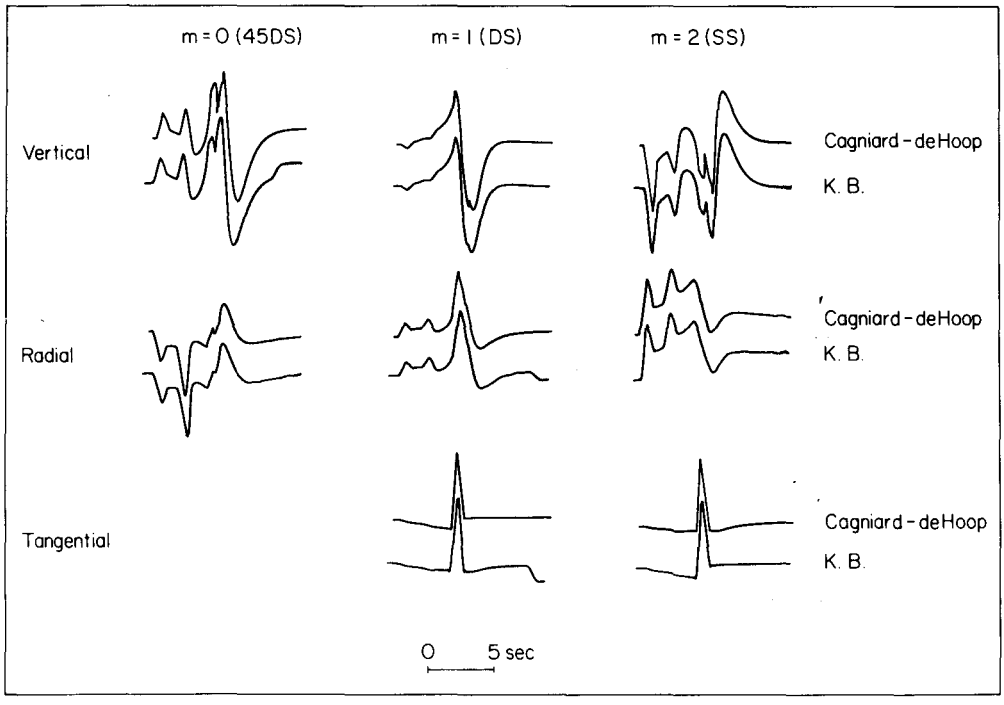

FIG. 4. Same as Figure 3, except the range is 32 km.

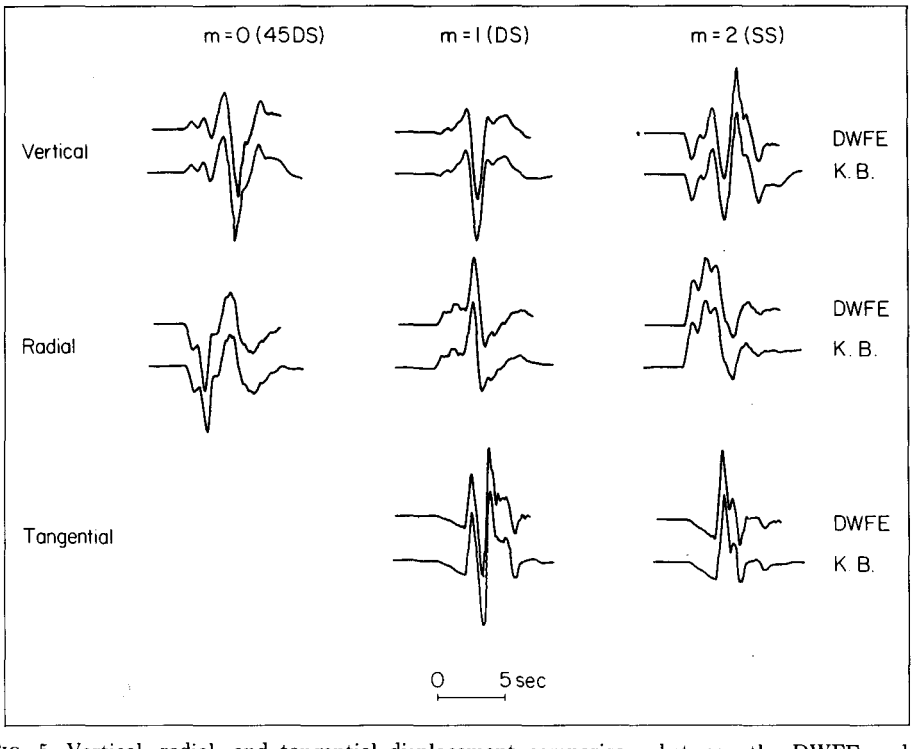

FIG. 5. Vertical, radial, and tangential displacement comparisons between the DWFE and KB techniques for a dislocation in a one layer over a half-space model. The records are for the three fundamental fault orientations at a range of 10 km. The source is in the upper layer at a depth of 2.5 km.

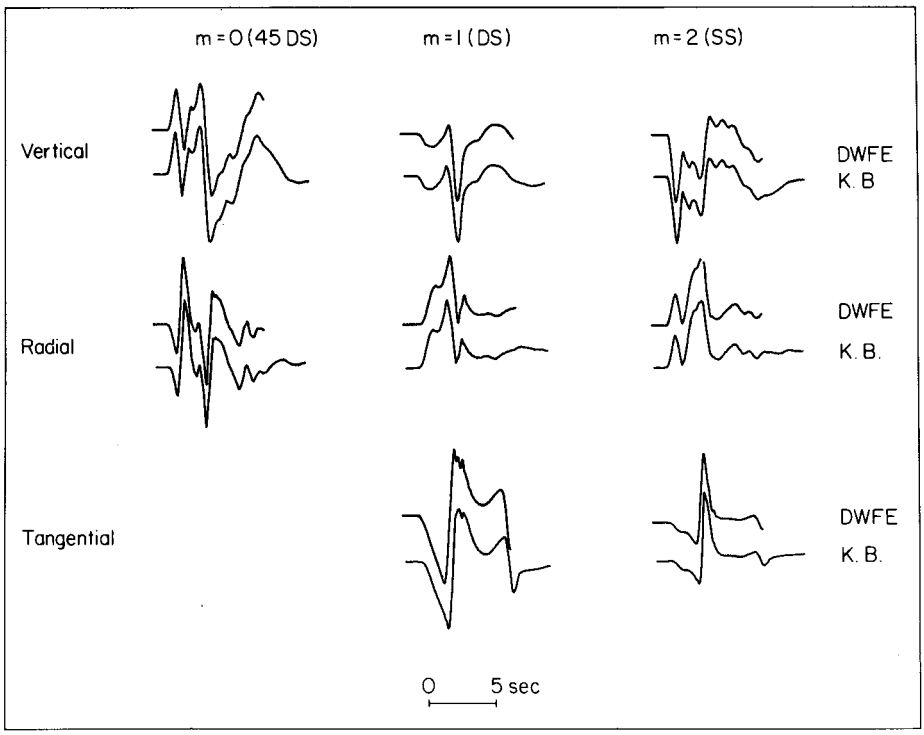

FIG. 6. Same as Figure 5, except the source is below the layer at a depth of 7 km.

is the displacement obtained with rays. The far-field source time function is a triangle with one second width, focal depth 8 km, the epicenter ranges are 16 km (Figure 3) and 32 km (Figure 4), respectively. The bottom traces are from the KB algorithm. The differences are very small and come mostly from the difference in time increments used in the two methods. In the generalized ray theory, we use $\Delta t = 0.03$ sec, in the other $\Delta t = 0.1$ sec.

For the layered half-space problem, we use solutions obtained by the DWFE method to check the KB result. Dislocation source displacements for a one layer half-space, with the source in the layer, $h = 2.5$ km, $r = 10$ are shown in Figure 5.

TABLE 3

LAYER PARAMETERS FOR THE ONE LAYER MODEL

h (km)	α (km/sec)	β (km/sec)	ρ (gm/cm^3)
5.0	3.500	2.000	2.400
∞	5.500	3.300	2.700

In Figure 6, the source is in the underlying medium, $h = 7.0$ km, $r = 10$ km. The layer model parameters are given in Table 3. The results of the two methods again show good agreement.

In Figure 7, we show a comparison between the KB and DWFE algorithms for an explosion at a depth of 1.2 km in an eight-layer model (Table 4) of the Amchitka crust over a mantle half-space. This structure was used to model the near-field records from the nuclear test event Milrow (Burdick, 1983). The synthetics are the free surface vertical particle velocities at ranges of 9.8 and 11.5 km. The nominal

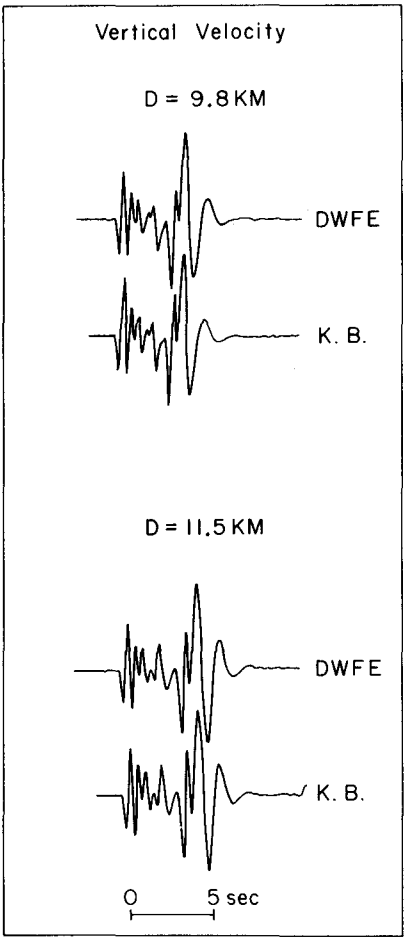

FIG. 7. Vertical velocity record comparisons between the DWFE and KB techniques for an explosion in the layered Millrow model. The Nyquist frequency is 5 Hz.

TABLE 4

LAYER PARAMETERS FOR THE MILROW MODEL

h (km)	α (km/sec)	β (km/sec)	ρ (gm/cm^3)
0.2	3.400	1.700	2.300
0.6	3.700	1.900	2.400
0.5	4.200	2.100	2.400
0.5	4.600	2.300	2.500
0.7	4.900	2.800	2.600
0.5	5.100	2.900	2.700
6.0	5.900	3.300	2.700
28.0	6.900	4.000	2.800
∞	8.200	4.700	3.200

maximum frequency in each synthetic is 5 Hz although the DWFE record is Butterworth filtered down to 5 Hz and the KB spectral calculation is truncated or terminated at 5 Hz. Because of this, the frequency content is slightly greater in the KB calculation. This difference can be seen in the relative excitation between the body waves and the Rayleigh wave pulse at the end of each synthetic. Considering their differences at high frequency, the time domain agreement is excellent.

For this model, 5 Hz is not sufficient to resolve *pP* from the direct *P* arrivals.

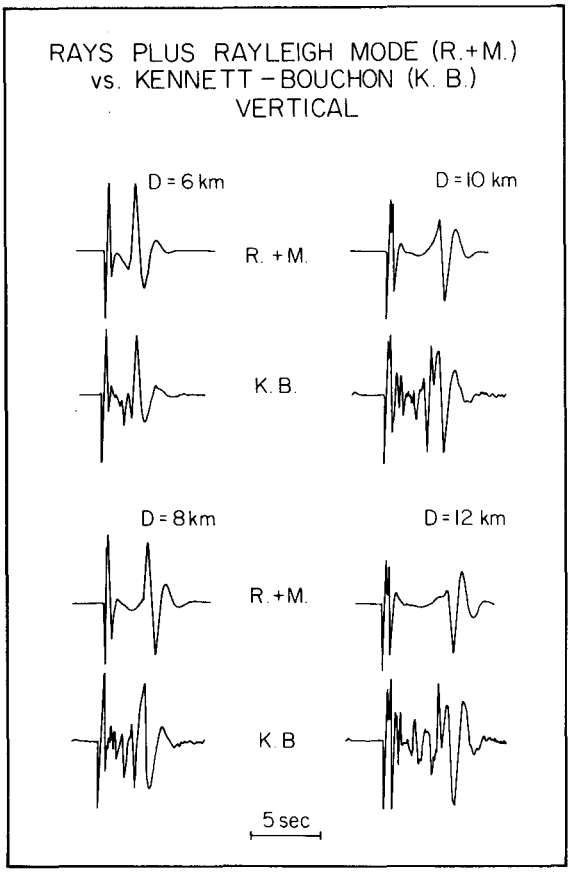

FIG. 8. Vertical velocity record comparisons between spliced ray-mode synthetics and the KB technique for an explosion in the layered Milrow model. The Nyquist frequency is 10 Hz.

Increasing the maximum frequency to 10 Hz, the *pP* arrival is seen in the double-peaked overswing following the direct *P* arrival at distances of 10 and 12 km on the vertical velocity KB record (Figure 8) and the radial velocity KB record (Figure 9). This identification was verified with the spliced generalized ray and modal synthetics appearing above the KB synthetics (Burdick, 1983) in Figures 8 and 9. The generalized ray sum (Helmberger, 1968) was restricted to direct and first multiple compressional waves. The only mode (Harkrider, 1964, 1970) used was the fundamental Rayleigh mode. With this structure, the 10-Hz DWFE calculation takes 10 times longer than the KB calculation.

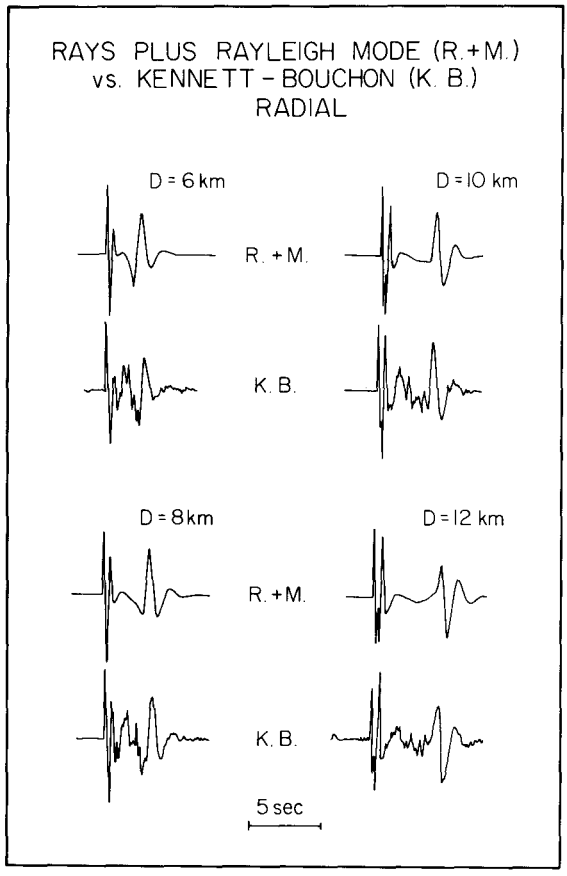

FIG. 9. Same as Figure 8, except the velocity records are radial.

CONCLUSIONS

We have presented a generalized reflection-transmission coefficient matrix and discrete wavenumber method for synthetic seismograms. For a dislocation source, the displacements on the free surface are represented as a linear combination of three fundamental shear dislocations. The wavenumber integrands are calculated by reflection and transmission coefficients, and the wavenumbers integration by discrete wavenumber summation method with complex frequencies which can yield accurate near-field static solutions.

Vertical integration schemes used in the near-field have been either spectral (Apsel, 1979; Bouchon, 1981) as in the regional techniques or finite-element (Olson, 1982) and finite-difference (Alekseev and Mikhailenko, 1980) in the time domain. The finite element schemes have the disadvantage in that the vertical step size is determined by the desired maximum frequency content, which in turn determines the time step required for stability. This time step is usually many times smaller than the time increment associated with the maximum frequency.

If portions of the vertical velocity and density profile are homogeneous, spectral techniques propagate across the region in one vertical step while the finite element-difference methods require many. On the other hand, in the vicinity of moderate vertical gradients, the step size or layer thickness of the spectral techniques will be at least as small as the finite-element difference scheme, and the number of

numerical operations are considerably more. In this situation, spectral techniques, in particular the KB method, are not as efficient as the time domain techniques. Convergence as the number of wavenumbers is increased is more straightforward using the spectral schemes and, as one would expect, the number of wavenumbers for a given convergence depends on the frequency being evaluated with fewer wavenumbers at the lower frequencies.

For the layered half-space problems presented, our results agree very well with synthetics generated by the Cagniard-de Hoop technique, *P-SV* modes, and the DWFE codes. For the 10-layered crust upper mantle model with a bandwidth of 0 to 10 Hz, this technique required only one-tenth the time of the DWFE calculation.

ACKNOWLEDGMENTS

This research was supported by the Advanced Projects Agency of the Department of Defense and was monitored by the Air Force Office of Scientific Research under Contract F49620-81-C-0008.

REFERENCES

Alekseev, A. S. and B. G. Mikhailenko (1980). Solution of dynamic problems of elastic wave propagation in inhomogeneous media by a combination of partial separation of variables and finite difference methods, *J. Geophys.* **48,** 161–172.

Apsel, R. J. (1979). Dynamic Green's functions for layered media and applications to boundary-value problems, *Ph.D. Thesis*, University of California, San Diego, California.

Bouchon, M. (1979). Discrete wave number representation of elastic wave fields in three-space dimensions, *J. Geophys. Res.* **84,** 3609–3614.

Bouchon, M. (1981). A simple method to calculate Green's functions for elastic layered media, *Bull. Seism. Soc. Am.* **71,** 959–971.

Burdick, L. J. (1983). Simultaneous modeling of body waves and surface waves in near field records of nuclear explosions, WCCP-R-83-02, Woodward-Clyde Consultants, Pasadena, California.

Fuchs, K. and G. Muller (1971). Computation of synthetic seismograms with the reflectivity method and comparison with observations, *Geophys. J. R. astr. Soc.* **23,** 417–433.

Harkrider, D. G. (1964). Surface waves in multilayered media. I. Rayleigh and Love waves from buried sources in a multilayered half-space, *Bull. Seism. Soc. Am.* **54,** 627–679.

Harkrider, D. G. (1970). Surface waves in multilayered elastic media. Part II. Higher mode spectra and spectral ratios from point sources in plane layered earth models, *Bull. Seism. Soc. Am.* **60,** 1937–1987.

Helmberger, D. V. (1968). The crust-mantle transition in the Bering Sea, *Bull. Seism. Soc. Am.* **58,** 179–214.

Helmberger, D. V. (1974). Generalized ray theory for shear dislocations, I., *Bull. Seism. Soc. Am.* **64,** 45–64.

Helmberger, D. V. and D. G. Harkrider (1978). Modeling earthquakes with generalized ray theory, in *Modern Problems in Elastic Wave Propagation*, J. Miklowitz and J. Achenbach, Editors, John Wiley and Sons, New York, 499–518.

Kennett, B. L. N. (1974). Reflections, rays, and reverberations, *Bull. Seism. Soc. Am.* **64,** 1685–1696.

Kennett, B. L. N. (1980). Seismic waves in a stratified half-space—II. Theoretical seismograms, *Geophys. J. R. astr. Soc.* **61,** 1–10.

Kennett, B. L. N and N. J. Kerry (1979). Seismic waves in a stratified half-space, *Geophys. J. R. astr. Soc.* **57,** 557–583.

Langston, C. A. and D. V. Helmberger (1975). A procedure for modelling shallow dislocation sources, *Geophys. J. R. astr. Soc.* **42,** 117–130.

Olson, A. H. (1982). Forward simulation and linear inversion of earthquake ground motions, *Ph.D. Thesis*, University of California, San Diego, California.

INSTITUTE OF GEOPHYSICS
ACADEMIA SINICA
BEIJING, PEOPLE'S REPUBLIC OF
CHINA (Z.X.Y.)

SEISMOLOGICAL LABORATORY
CALIFORNIA INSTITUTE OF TECHNOLOGY
PASADENA, CALIFORNIA 91125 (D.G.H.)
CONTRIBUTION NO. 3889

Manuscript received 24 March 1983

APPENDIX

The relations for phase normalized reflection and transmission coefficients are as follows

$$\begin{aligned}
\tilde{\mathbf{r}}^D_{PP} &= e^{-2ad}\mathbf{r}^D_{PP} & \tilde{\mathbf{t}}^D_{PP} &= e^{-ad}\mathbf{t}^D_{PP}\\
\tilde{\mathbf{r}}^D_{SP} &= e^{-(a+b)d}\mathbf{r}^D_{SP} & \tilde{\mathbf{t}}^D_{SP} &= e^{-bd}\mathbf{t}^D_{SP}\\
\tilde{\mathbf{r}}^D_{PS} &= e^{-(a+b)d}\mathbf{r}^D_{PS} & \tilde{\mathbf{t}}^D_{PS} &= e^{-ad}\mathbf{t}^D_{PS}\\
\tilde{\mathbf{r}}^D_{SS} &= e^{-2bd}\mathbf{r}^D_{SS} & \tilde{\mathbf{t}}^D_{SS} &= e^{-bd}\mathbf{t}^D_{SS}\\
\tilde{\mathbf{r}}^U_{PP} &= \mathbf{r}^U_{PP} & \tilde{\mathbf{t}}^U_{PP} &= e^{-ad}\mathbf{t}^U_{PP}\\
\tilde{\mathbf{r}}^U_{SP} &= \mathbf{r}^U_{SP} & \tilde{\mathbf{t}}^U_{SP} &= e^{-ad}\mathbf{t}^U_{SP}\\
\tilde{\mathbf{r}}^U_{PS} &= \mathbf{r}^U_{PS} & \tilde{\mathbf{t}}^U_{PS} &= e^{-bd}\mathbf{t}^U_{PS}\\
\tilde{\mathbf{r}}^U_{SS} &= \mathbf{r}^U_{SS} & \tilde{\mathbf{t}}^U_{SS} &= e^{-bd}\mathbf{t}^U_{SS}
\end{aligned}$$

where

$$\hat{R}_D = \begin{pmatrix} \tilde{\mathbf{r}}^D_{PP} & \tilde{\mathbf{r}}^D_{PS} \\ \tilde{\mathbf{r}}^D_{SP} & \tilde{\mathbf{r}}^D_{SS} \end{pmatrix}$$

with similar matrix indexing for $\hat{R}_U$, $\hat{T}_D$, and $\hat{T}_D$.

For the interface reflection and transmission coefficients, say from layer 1 to layer 2, we have

$$\begin{aligned}
\mathbf{r}^D_{PP} &= [k^2a_1b_1a_2b_2(\mu_2-\mu_1)^2 - k^2(\mu_1\Omega_1-\mu_2\Omega_2)^2 - a_1b_1(\mu_2\Omega_2-k^2\mu_1)^2\\
&\quad + a_2b_2(\mu_1\Omega_1-k^2\mu_2)^2 - \tfrac{1}{4}\mu_1\mu_2k^2_{\beta_1}k^2_{\beta_2}(a_1b_2-b_1a_2)]/\Delta_1\\
\mathbf{r}^D_{SP} &= -2kb_1[(\mu_2\Omega_2-k^2\mu_1)(\mu_1\Omega_1-\mu_2\Omega_2) - a_2b_2(\mu_2-\mu_1)(\mu_1\Omega_1-k^2\mu_2)]/\Delta_1\\
\mathbf{r}^D_{PS} &= \frac{a_1}{b_1}\mathbf{r}^D_{SP}\\
\mathbf{r}^D_{SS} &= [k^2a_1b_1a_2b_2(\mu_2-\mu_1)^2 - k^2(\mu_1\Omega_1-\mu_2\Omega_2)^2 - a_1b_1(\mu_2\Omega_2-k^2\mu_1)^2\\
&\quad + a_2b_2(\mu_1\Omega_1-k^2\mu_2)^2 + \tfrac{1}{4}\mu_1\mu_2k^2_{\beta_1}k^2_{\beta_2}(a_1b_2-b_1a_2)]/\Delta_1\\
\mathbf{t}^D_{PP} &= \mu_1k^2_{\beta_1}a_1[(\mu_2\Omega_2-k2\mu_1)b_1 + (\mu_1\Omega_1-k^2\mu_2)b_2]/\Delta_1\\
\mathbf{t}^D_{SP} &= \mu_1k^2_{\beta_1}b_1[(\mu_2-\mu_1)a_1b_2 + (\mu_1\Omega_1-\mu_2\Omega_2)]/\Delta_1\\
\mathbf{t}^D_{PS} &= \mu_1k^2_{\beta_1}a_1[(\mu_2-\mu_1)b_1a_2 + (\mu_1\Omega_1-\mu_2\Omega_2)]/\Delta_1\\
\mathbf{t}^D_{SS} &= \mu_1k^2_{\beta_1}b_1[(\mu_2\Omega_2-k^2\mu_1)a_1 + (\mu_1\Omega_1-k^2\mu_2)a_2]/\Delta_1
\end{aligned}$$

and

$$\begin{aligned}
\Delta_1 &= [k^2a_1b_1a_2b_2(\mu_2-\mu_1)^2 + k^2(\mu_1\Omega_1-\mu_2\Omega_2)^2 - a_1b_1(\mu_2\Omega_2-k^2\mu_1)^2\\
&\quad - a_2b_2(\mu_1\Omega_1-k^2\mu_2)^2 - \tfrac{1}{4}\mu_1\mu_2k^2_{\beta_1}k^2_{\beta_2}(a_1b_2+b_1a_2)]
\end{aligned}$$

where Δ_i is the Stoneley wave equation for the interface between layers i and $i+1$.

For R_U and T_U we have

$$\mathbf{r}_{PP}^{U} = [k^2 a_1 b_1 a_2 b_2(\mu_2 - \mu_1)^2 - k^2(\mu_1\Omega_1 - \mu_2\Omega_2)^2 + a_1 b_1(\mu_2\Omega_2 - k^2\mu_1)^2$$
$$-a_2 b_2(\mu_1\Omega_1 - k^2\mu_2)^2 + \tfrac{1}{4}\mu_1\mu_2 k_{\beta_1}^2 k_{\beta_2}^2(a_1 b_2 - b_1 a_2)]/\Delta_1$$

$$\mathbf{r}_{SP}^{U} = 2kb_2[(\mu_1\Omega_1 - k^2\mu_2)(\mu_2\Omega_2 - \mu_1\Omega_1) - a_1 b_1(\mu_1 - \mu_2)(\mu_2\Omega_2 - k^2\mu_1)]/\Delta_1$$

$$\mathbf{r}_{PS}^{U} = \frac{a_2}{b_2}\,\mathbf{r}_{SP}^{U}$$

$$\mathbf{r}_{SS}^{U} = [k^2 a_1 b_1 a_2 b_2(\mu_2 - \mu_1)^2 - k^2(\mu_1\Omega_1 - \mu_2\Omega_2)^2 + a_1 b_1(\mu_2\Omega_2 - k^2\mu_1)^2$$
$$-a_2 b_2(\mu_1\Omega_1\ k^2\mu_2)^2 - \tfrac{1}{4}\mu_1\mu_2 k_{\beta_1}^2 k_{\beta_2}^2(a_1 b_2 - b_1 a_2)]/\Delta_1$$

$$\mathbf{r}_{PP}^{U} = \frac{\rho_2 a_2}{\rho_1 a_1}\,\mathbf{t}_{PP}^{D}$$

$$\mathbf{t}_{PS}^{U} = \frac{\rho_2 a_2}{\rho_1 b_1}\,\mathbf{t}_{PS}^{D}$$

$$\mathbf{t}_{SP}^{U} = \frac{\rho_2 b_2}{\rho_1 a_1}\,\mathbf{t}_{SP}^{D}$$

$$\mathbf{t}_{SS}^{U} = \frac{\rho_2 b_2}{\rho_1 b_1}\,\mathbf{t}_{SS}^{D}.$$

For *SH* waves

$$\mathbf{r}_{SH}^{D} = \frac{\mu_1 b_1 - \mu_2 b_2}{\mu_1 b_1 + \mu_2 b_2}$$

$$\mathbf{t}_{SH}^{D} = \frac{2\mu_1 b_1}{\mu_1 b_1 + \mu_2 b_2}$$

$$\mathbf{r}_{SH}^{U} = \frac{\mu_2 b_2 - \mu_1 b_1}{\mu_1 b_1 + \mu_2 b_2}$$

$$\mathbf{t}_{SH}^{U} = \frac{2\mu_2 b_2}{\mu_1 b_1 + \mu_2 b_2}.$$